PNAS

Supplementary Information for

Hot and dry conditions predict shorter nestling telomeres in an endangered songbird: implications for population persistence

Justin R. Eastwood[1,9], Tim Connallon[1], Kaspar Delhey[1,2], Michelle L. Hall[3,4,5], Niki Teunissen[1], Sjouke A. Kingma[6,7], Ariana M. La Porte[1], Simon Verhulst[8], Anne Peters[1,6].

[1] School of Biological Sciences, Monash University, 25 Rainforest Walk, Clayton, Victoria 3800, Australia.
[2] Department Behavioural Ecology & Evolutionary Genetics, Max Planck Institute for Ornithology, Eberhard Gwinnerstr., 82319 Seewiesen, Germany.
[3] Bush Heritage Australia, 395 Collins Street, Melbourne, Vic 3000, Australia.
[4] School of BioSciences, University of Melbourne, Melbourne, Parkville, Victoria 3010, Australia.
[5] School of Biological Sciences, University of Western Australia, Crawley, WA 6009, Australia.
[6] Max Planck Institute for Ornithology, Vogelwarte Radolfzell, Schlossallee 2, 78315 Radolfzell, Germany.
[7] Behavioural Ecology Group, Department of Animal Sciences, Wageningen University and Research, De Elst 1, 6708 WD Wageningen, The Netherlands.
[8] Groningen Institute for Evolutionary Life Sciences, University of Groningen, Nijenborgh 7, 9747 AG Groningen, Netherlands.
[9] Correspondence: justin.eastwood@monash.edu

Table of Contents

Supplementary information appendix

Supplementary materials and methods

(I) Telomere measurement: additional information.

Nest monitoring and sample collection.

Between 2007-2011 and 2016-2018, social groups were checked weekly for signs of nesting, and once found, nests were checked every three days (1–3). At seven days after hatching (range 4-9), nestlings were banded with a unique combination of colour bands and a numbered metal band from the Australian Bird and Bat Banding Scheme. For DNA analysis, blood was taken from the brachial vein using a 25g needle and a heparinised capillary tube which was then centrifuged (4, 5). For individuals bled in 2007-2011, red blood cells were stored in Longmire's lysis buffer and in 2016-2018 red blood cells were stored in 100% ethanol. Samples were stored at 4°C until processed in the laboratory.

Quantifying telomere length.

To extract high quality DNA, we used a modified QIAamp DNA kit (Qiagen) and automated the process using a QIAcube HT instrument. DNA purity and concentration was assessed using a NanoDrop (ND-1000) and DNA integrity was assessed on an agarose gel (5).

A qPCR method based on Criscuolo et al., (6) and validated for use in *M. coronatus* by Eastwood et al., (5) was used to measure telomere length (TL) relative to a control gene. In brief, qPCR reactions were prepared by automation in an EpMotion 5075 on 96-well plates. The total reaction volume of 25 µl included 12.5 µl of SYBR Green I (Roche), 300 nM of both the normalising control gene (glyceraldehyde-3-phoshate dehydrogenase; GAPDH) primers or 400 nM of both telomere primers (Integrated DNA Technologies) and 10 ng of sample DNA (except the two-fold serial dilution containing 40, 20, 10, 5 and 2.5 ng of DNA). Samples and controls were run in duplicate. The telomere primers were Tel1b 5' - CGG TTT GTT TGG GTT TGG GTT TGG GTT TGG GTT TGG GTT - 3' and Tel2b 5' - GGC TTG CCT TAC CCT TAC CCT TAC CCT TAC CCT TAC CCT - 3' (8). The GAPDH primers were GT2-GAPDH-forward 5' - CCA TCA CAG CCA CAC AGA AG - 3' and GT2-GAPDH-reverse 5' - TTT TCC CAC AGC CTT AGC AG - 3' (7). Reactions were run on a LightCycler 480 (Roche) machine on separate plates as follows: telomere (95°C for 15 minutes, followed by 35 cycles of 15 seconds at 95°C, 30 seconds at 56°C, 30 seconds at 72°C) and GAPDH (95°C for 15 minutes, followed by 40 cycles of 15 seconds at 95°C, 30 seconds at 60°C, 30 seconds at 72°C). A melt-curve analysis followed both reactions to ensure the correct product was amplified. Efficiencies and intra- and

inter-assay repeatabilities were high (5). qPCR quality control and the calculation of relative telomere length were as Eastwood *et al*., (5).

Using unscaled relative TL estimates, variation in this study's dataset and that described in Eastwood et al. 2019 are comparable with overlapping distributions. This study: mean = 1.18, sd = 0.18, min = 0.59, max = 1.72. Eastwood et al. 2019: mean = 1.24, sd = 0.15, min = 0.87, max = 1.56.

(II) Statistical analysis: additional information.

The statistical analysis investigating temperature related effects on early-life telomere length included controlling variables accounting for individual, ecological, and methodological factors that may also explain early-life telomere length. Below we discuss our justifications for including them in the statistical model and provide additional methodological details.

Individual factors: age, sex and body size.

It was necessary to control for age at sampling because it was not feasible to sample all nests on day seven. In other species, telomere shortening rate is faster during nestling growth period due to the high rates of cell replication (8). Therefore, large differences between nestlings may occur within short time periods (sampling completed between 4-9 days). Similarly, body mass (mean = 7.77 ± 1.11 sd g) and tarsus length (mean = 17.44 ± 1.95 sd mm) are included in the model to account for body size variation. Body size has been associated with nestling telomere length in other species (8, 9) and is related through either variability in growth and cell replication or body condition. Sex differences in telomere length are also well documented across the tree of life (10), and necessary to control for in the analysis.

Nest level factors: parental effects, group size, brood size and year.

Purple-crowned fairy-wrens are cooperative breeders (1, 11, 12), where subordinate group members help the dominant breeding pair raise offspring and defend the territory against predators and interlopers (3, 13, 14). Previous work in this species demonstrated that territories with more helpers provisioned nestlings at higher rates and fledge more young (11). The variability of care between territories with different group sizes may contribute to nestling telomere variation. In addition, cooperative breeding may be able to compensate for environmental stressors (15, 16, but see 17) for an example where group size was not able to compensate under hot conditions). Therefore, we include group size as a controlling factor. The number of helpers within a group varies (categorical: 0, 1, 2 and 3+), with the category 3+ rare in this population (<10%; although this percentage may fluctuate with population size). Over the study period (2008-2021), there is a weak

relationship between the number of groups with 3+ helpers within a territory and annual population size (scaled; regression estimate = 0.06, se = 0.02, P = 0.04).

Brood size is known to negatively affect TL, and has been demonstrated experimentally by manipulating brood size (18–20). Therefore, brood size (nest mean = 2.53 ± 0.84, median = 3, range = 1-4 nestlings) was also included as a covariate as it controls for potential costs related to the number of nestlings.

We included maternal and paternal ID as random effects in the linear mixed effects model to account for parental experience, genetic or epigenetic effects (21–24). Nest ID was included as a random effect to control for the independence of nesting environment. Paternal ID as a random factor explained less than 1% of the variance and was subsequently removed from further analyses. It is also conceivable that year (Austral year, running from June to July) could account for possible cohort effects independent of the weather variables, T_{max}, T_{min}, season and rainfall. However, due to our sampling structure and the high correlation between year and weather, the inclusion of year as a random term was not feasible without producing spurious results. Although, the conclusions remained similar.

Methodological factors: blood storage buffer and qPCR plate.

The qPCR method used to measure telomere length in this study was previously optimised for use in purple-crowned fairy-wrens (5). Eastwood et. al. (5), found that telomere length varied according to which blood storage buffer was used. Telomeres were longer on average when blood was stored in ethanol compared to Longmire's buffer. Therefore, blood storage buffer was included in the model as a fixed factor to control for mean differences between samples stored in Longmire's buffer or ethanol.

In addition, qPCR plate ID was included in the model to account for reaction variation between each qPCR run. Multiple runs were necessary because of the limited number of samples that fit on each plate.

Territory quality.

Habitat and the conditions where individuals develop are likely to explain a proportion of telomere length variation (24). In this study, territory quality was based on an estimate of *Pandanus aquaticus* cover in each territory because *M. c. coronatus* is completely dependent on this vegetation for habitat (4, 12, 25–27). As previously described, at each territory an observer assigned a Pandanus quality score between 0 and 10 for each bank of the river every 50m, scores for both sides were then combined to create a score of 0 to 20. A total score of 0 for one bank indicates absence of Pandanus, a score of ~10 indicates patchy Pandanus (~$14m^2$ of mature Pandanus per 20m of river/creek), a score of ~20 indicates high-quality dense Pandanus (~$50m^2$ of mature Pandanus per 20m of

river/creek)(4, 27). Scores were then spatiotemporally matched with territories using QGIS (version 2.18.16). Territory quality was measured intermittently during the study period (4, 12) but was relatively stable within each territory, changing slowly over time. Therefore, missing values were interpolated. For this study, scores were averaged into a single score for each territory per year. Territory quality was included in the linear mixed effects model as a fixed covariate and in an interaction with average maximum temperature (T_{max}) to account for possible buffering effects of the Pandanus vegetation. Territory quality varied substantially, and averaged 10.9 ± 5.1 sd, range 0-19 unit scores. Previous work has shown that this method of territory quality scoring is biologically important as lower territory quality has been associated with a higher risk of nest failure (28), and females may divorce partners to move to a higher quality territory (27). Moreover, territory quality affects male and female phenotype (colour; (29–31)), although these effects are quite subtle compared to the effect on nest failure.

Feeding rate and average prey size.

Nutrition is associated with growth and condition which could influence telomere dynamics (32). Altricial nestlings are wholly dependent on parental provisioning, which declines when conditions are hot and dry both because prey becomes more elusive and parental activity is reduced (33). Hence, we determined parental provisioning rate and average prey size of items delivered to nestlings for all nests, as previously described (1, 3, 11). Observers were concealed approximately 10 m away and watched for one hour while recording the number of visits. A feed was recorded when a bird approached the nest and appeared to feed one of the nestlings. Each nest was observed 2.85 times on average (standard deviation = 1.12) and usually on consecutive days. Observations took place either in the early morning (am; between 0530 and 1130) or afternoon (pm; 1400 to 1800). Nestlings were between 4 and 10 days old during the nest watches (34). To control for this variation in nest observations we fitted a linear mixed effects model and included feeding rate per nestling as the dependent variable. Nest id was included as a random effect with time of day (am/pm) and age of nestlings as fixed effects. An interaction between the fixed effects was included because females tended to brood young nestlings in the mornings (34). Provisioning rate repeatability was ICC = 0.46. The model predicted values were saved without the random effect and averaged for each nest (hereafter, 'provisioning rate'). These values were then included in the primary analyses predicting nestling telomere length (provisioning rate average = 5.14 ± 1.50 sd number of feeds per hour per nestling). Provisioning rate was included in the linear mixed effects model as a fixed covariate. In addition to provisioning rate, the amount of nutrition provided to the nestlings may vary with the size of prey items. During nest observations, whenever possible, the size of the food (invertebrates) was noted relative to the size of the bill of the bird providing food. The prey size estimates were

then averaged (average prey size: average 1.19 ± 0.35 sd prey size relative to feeder bill). Average prey size was included in the model as a fixed covariate.

Excluding nests with extra pair offspring.

The *Malurus* genus is known for high rates of extra-pair paternity (EPP) (35). However, purple-crowned fairy-wrens are one exception with less than 5% EPP in the wild (36, 37). Therefore, the number of nests with EPP was low and these were excluded from this study because of the lack of statistical power to detect any relationship with telomere length. Genetic microsatellite identification and parentage analysis to identify extra-pair young are described in (27).

(III) Relationship between air temperature and nest temperature.

In this study, we used air temperatures (T_{max} and T_{min}) from nearby weather stations as predictors in our analyses (see materials and methods). These estimates are broad indicators of local temperature. However, it is important to understand how much variation exists between air temperature and temperature experienced within the nest (i.e. the microclimate). Nestling purple-crowned fairy-wrens may experience different microclimates due to variation in vegetation, nest position and construction, or territory location, which may not necessarily be reflected in ambient air temperatures measured from weather stations. Therefore, we conducted a study to investigate the relationship between weather station air temperature and nest temperature.

To assess the relationship between air temperature and in-nest temperature, black bulb thermometers (hereafter black bulbs, n = 46) were placed in empty nests after nestlings had either fledged or the nest had failed from February – July in 2021. Black bulbs are matte black copper spheres, 0.8mm x 30 mm in diameter, containing a DS1921G-F5# Thermochron iButton (Sunnyvale, CA, USA) (hereafter iButtons). They were placed as soon as nests were empty and left for between 6-8 days, after which the data was downloaded using a DS1402D-DR8+ iButton Reader with a LinkUSB - 1-Wire USB Interface adaptor. iButtons recorded temperature in 20 minute intervals. Black bulb measurements do not reflect the exact temperature experienced by nestlings, as this would include metabolic heat production, the influence of their nest-mates, parental brooding, and plumage. Rather, black bulbs provide a body with standard thermal properties that incorporate the effect of wind and solar radiation into a single temperature measurement (38, 39). They are therefore appropriate to compare microclimates (40, 41) such as nest interiors. Assessment of maximum temperatures recorded in nests revealed that during daylight hours, black bulbs occasionally spike in temperature for short periods, but these spikes do not appear at night. Spikes were presumably

caused by a fleeting exposure of the black bulbs to solar radiation, possibly through the nest opening or holes in the top of the nest. Because this analysis concerns the microclimate rather than the magnitude of brief temperature spikes, which do not reflect nest microclimate, mean daily temperature during the hottest part of the day (12:00 to 15:00) was used as a metric of maximum daily nest temperature. This metric and daily maximum temperature from local weather stations (calculated as previously described, see materials and methods) were averaged over the in-nest sampling period (T_{max_nest} and T_{max_air}, respectively). In a linear regression model, we assessed the relationship between T_{max_nest} (dependent variable, $\log_{10}$ transformed to improve normality of the model residuals) and T_{max_air} whilst controlling for three environmental conditions: Wet season with rain, Wet season without rain, and Dry season without rain. No data were available during the Dry season with rain. We also included an interaction between T_{max_air} and environmental condition to test whether the direction or magnitude of the relationship between nest and air temperature varies with environment. Furthermore, we performed a second model using a similar structure but replacing the temperature variables with T_{min_nest} (dependent variable; in-nest average daily minimum temperature °C) and T_{min_air} (independent variable; weather station average daily minimum temperature °C). However, model interactions were not significant ($P > 0.05$) and were removed from the regression. T_{max_air} and T_{min_air} significantly predicted T_{max_nest} and T_{min_nest}, respectively ($P < 0.001$, *SI appendix* Table S2 and Fig. S3), confirming that the use of air temperature in this study broadly reflects the temperatures nestlings experience within the nest.

(IV) *Post hoc* statistical analysis of potential confounding variables and mechanisms.

Because the effect of high temperature on nestling TL (Table 1) could possibly be (partly) explained by broader ecological or social factors, we decided to explore possible alternative mechanisms or confounding interactions that could explain these findings.

Social and environmental interactions.

Temperature may interact with ecological and social variables in a way that can either mitigate or exacerbate the effects of temperature on nestling telomere length. However, despite having a large sample size we lack the statistical power to include all possible interactions in the model simultaneously. We therefore adopted an approach where each interaction was included in the LMM Table 1 separately as a *post hoc* test to identify possible associations for future research. The following variables were included in an interaction with temperature: food provisioning rate, which tests for possible differences in feeding rate under hot conditions (42); the number of helpers, which tests for potential compensation of larger groups under suboptimal conditions (17); brood size and temperature, because larger broods could have a reduced capacity to thermoregulate within nests;

sex, as temperatures may differentially influence males and females; and territory quality, because the amount of vegetation may affect microclimate or other factors. No interactions were found to be significant ($P > 0.26$). It is conceivable that three-way interactions or greater are biologically plausible. However, they were not included in the model because the required sample size is not currently feasible.

Parental TL effects on nestling TL.

Parental TL at the time of breeding may account for variation in nestling TL. In addition, it may confound the effects of temperature and season if parental TL is related to the timing of breeding. We conducted a *post hoc* examination of this by including maternal and paternal TL into the final model presented in Table 1, thereby controlling for parental TL directly. From 175 nests, telomere measurements were available from n= 116 mothers and n = 118 fathers (234 out of 350 total parents), with n = 100 nests having both parents sampled. Telomeres were measured using the same qPCR method described above. We used the closest parental TL measure within one year to nestling hatch date. To account for methodological variation, we used the predicted parental TL values from a linear mixed effects model including relative TL as the dependent variable, qPCR run ID as a random effect and blood storage buffer as a fixed factor. Maternal and Paternal TL were each scaled to have a mean of zero and standard deviation of one. Missing values were replaced with zero so that the full dataset and model could be compared. Maternal and Paternal TL were then re-scaled.

When controlling for maternal and paternal TL as covariates in the statistical model, the conclusions of this study did not change. The effect of temperature and its interactions with season and rainfall remained highly similar and significant (*SI appendix* Table S1). Neither maternal nor paternal TL were significantly associated with nestling TL. Based on AIC values the original model is more parsimonious ($AIC_c = 1147.68$) compared to the model including parent TL ($AIC_c = 1154.53$), delta $AIC_c = 6.85$. Therefore, we have retained our original model in the main manuscript and present these findings in Table S1.

Supplementary results

(V) Supplementary figures

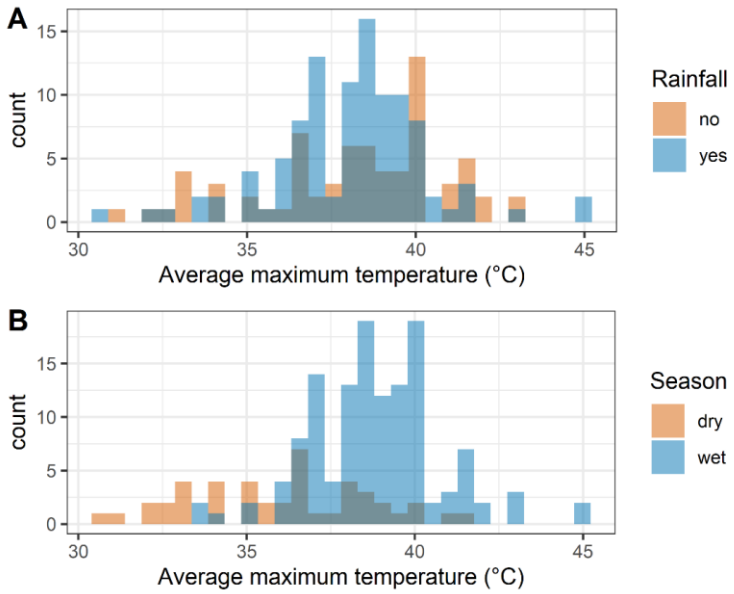

Figure S1: Frequency of average T_{max} over the nestling period (n = 175 nests). Organised by **A)** whether it rained during the nestling period, or **B)** whether nesting was during the wet or dry season.

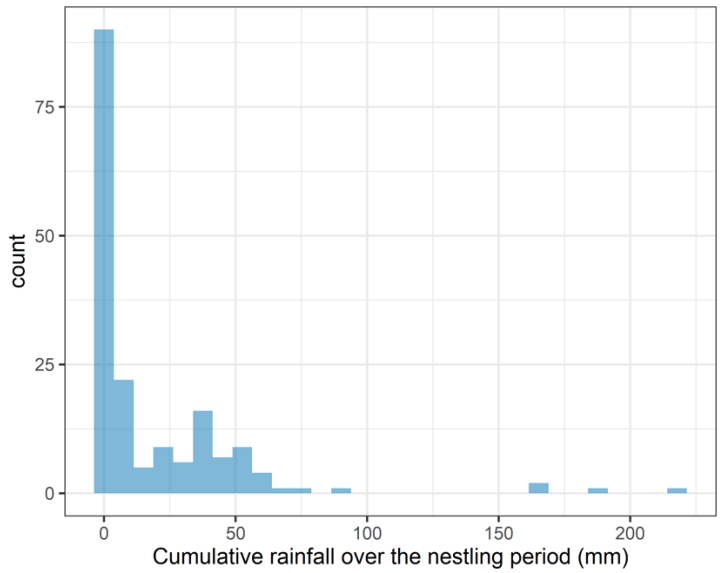

Figure S2: Frequency distribution of cumulative rainfall over the nestling period (n = 175 nests).

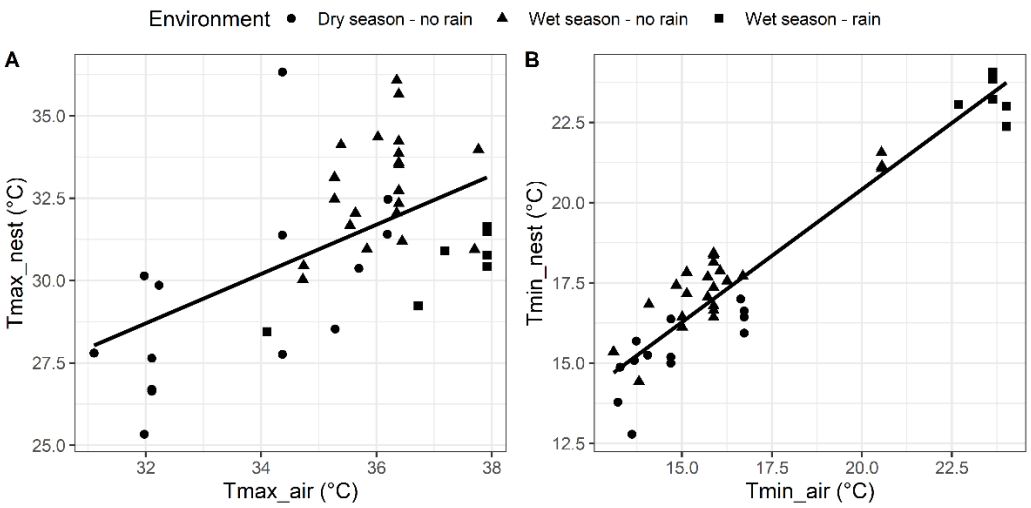

Figure S3: Air temperature predicts nest temperature. A) shows the positive relationship between T_{max_nest} (mean black bulb temperatures between 12:00 to 15:00 each day, averaged over deployment period) and T_{max_air} (average maximum daily air temperature recorded from nearby weather stations over the same period). B) shows the positive relationship between T_{min_nest} (average daily black bulb minimum temperature over deployment period) and T_{min_air} (average minimum daily air temperature recorded from nearby weather stations over the same period). Linear regression models confirm that air temperatures are strongly predicted by nest temperatures ($P<0.001$, Table S2).

(VI) Supplementary tables

Table S1: Maternal and paternal telomere length have no effect on early-life TL (n = 417 individuals) when inserted into the environmental determinants model from Table 1. Parental telomere lengths were estimated within a year from conception of the nestlings. Shown are results from the linear mixed effects model with TL (z-score transformed) as dependent variable; all continuous explanatory variates were mean centred. Daily maximum (T_{max}) and minimum temperature (T_{min}) were averaged across the nestling period (from hatching to day seven). Bold indicates significant predictors ($p<0.05$). Model residuals and predictor covariance estimates were examined to confirm that the model assumptions were met. AIC_c = 1155.53, including fixed predictors only R^2_m = 0.09, including random and fixed predictors R^2_c = 0.62.

Parameter	Estimate (se)	df	t	p
Intercept	-0.147 (0.277)	153.039	-0.531	0.596
T_{max}	**-0.157 (0.048)**	**123.685**	**-3.266**	**0.001**
T_{min}	-0.006 (0.028)	130.374	-0.230	0.819
Rainfall (Rain)	0.156 (0.161)	140.732	0.971	0.333
Season (wet)	0.090 (0.193)	124.855	0.466	0.642
Rainfall (Rain) × T_{max}	**0.101 (0.047)**	**141.648**	**2.136**	**0.034**
Season (wet) × T_{max}	**0.133 (0.062)**	**156.615**	**2.149**	**0.033**
Maternal telomere length	-0.033 (0.058)	145.102	-0.563	0.574
Paternal telomere length	0.062 (0.060)	163.067	1.041	0.299
Parental provisioning rate	**0.094 (0.048)**	**173.958**	**1.973**	**0.050**
Prey size	0.070 (0.176)	139.097	0.399	0.691
Territory quality	0.021 (0.016)	112.599	1.351	0.180
Number of helpers (1)	0.072 (0.129)	130.534	0.555	0.580
(2)	-0.122 (0.165)	150.156	-0.739	0.461
(3+)	**-0.549 (0.187)**	**114.169**	**-2.937**	**0.004**
Sex (male)	**0.204 (0.079)**	**343.311**	**2.572**	**0.011**
Mass (g)	-0.124 (0.078)	351.646	-1.579	0.115
Tarsus length (mm)	0.026 (0.048)	353.323	0.539	0.591
Brood size (range 1-4)	0.046 (0.075)	153.721	0.613	0.541
Age at sampling (5-9 days)	0.073 (0.067)	194.101	1.089	0.277
Blood storage buffer (Longmire's)	0.052 (0.236)	102.640	0.218	0.828
Variance components (sd)				
Nest ID	0.084 (0.289)			
Maternal ID	0.312 (0.559)			
qPCR Run ID	0.232 (0.481)			
Residual	0.445 (0.667)			

Table S2: Air temperatures predict in-nest temperatures. Model A includes T_{max_nest} as dependent variable and T_{max_air}, environmental condition, and their interaction as predictor variables. Model B replaces maximum temperature variables with T_{min_nest} as the dependent variable with T_{min_air} as a predictor variable. Note, the interactions between season and air temperature (T_{max_air} and T_{min_air}) were not significant and were removed from each final model.

Parameter	Estimate (se)	t	p
Model A: $Log_{10}(T_{max\_nest})$			
Intercept	2.507 (0.228)	11.000	<0.001
T_{max_air}	**0.026 (0.007)**	**3.832**	**<0.001**
Season (Wet without rain)	0.042 (0.026)	1.628	0.111
Season (Wet with rain)	-0.054 (0.035)	-1.526	0.135
Season (Wet without rain) × T_{max_air}	-0.018 (0.017)	-1.079	0.287
Season (Wet with rain) × T_{max_air}	-0.006 (0.019)	-0.307	0.761
Model B: $Log_{10}(T_{min\_nest})$			
Intercept	2.595 (0.062)	33.621	<0.001
T_{min_air}	**0.043 (0.005)**	**10.497**	**<0.001**
Season (Wet without rain)	**0.077 (0.015)**	**5.013**	**<0.001**
Season (Wet with rain)	0.039 (0.041)	0.952	0.346
Season (Wet without rain) × T_{min_air}	-0.001 (0.010)	0.088	0.930
Season (Wet with rain) × T_{min_air}	-0.052 (0.041)	-1.257	0.216

(VII) Evolutionary modelling: parameter estimates.

Table S3: Estimates for each water availability condition used in the evolutionary modelling and an explanation of how they were derived. A breakdown of the observed effect of maximum temperature (T_{max}) on nestling telomere length (TL) for each of the four water availability conditions (p_1, p_2, p_3, and p_4) was obtained from the model presented in Table 1. N is the number of nestlings and *p* the proportion of nestlings in each of the four conditions. The weighted effect sizes were calculated by multiplying the proportion of nestlings with the effect size of T_{max}. The proportions of nestlings in each category, $N_{current}$ were calculated using only years when both the complete Wet and complete Dry season were sampled to avoid any sampling bias. The overall weighted effect of T_{max} on TL is the sum of weighted effect sizes which equals -0.008. A projected estimate for the future number of nestlings to experience each of the four environmental conditions, N_{future}, was calculated according to rainfall projections for the Kimberley region found in Moise *et al.* (43). Wet season rainfall is estimated to increase by 3% whilst Dry season rainfall is expected to decrease by 15%. Therefore, we adjusted the number of nestlings within each season according to those values. i.e., Wet season with rainfall +3%, Wet season without rainfall -3%, Dry season without rainfall +15%, and Dry season with rainfall -15%. On top of that, the two categories without rainfall were increased by a further 20% and the categories with rainfall reduced by 20%. This 20% approximately adjusts for predictions that the number of days without rain will increase.

Water availability condition	Season (Wet/Dry)	Rainfall (yes/no)	β_T (se)	$N_{current}$	$P_{current}$	Weighted $\beta_{T^{current}}$	N_{future}	Weighted $\beta_{T^{future}}$
P_1	Dry	No	-0.156 (0.049)	54	0.23	-0.036	74	-0.050
P_2	Dry	Yes	-0.055 (0.055)	20	0.09	-0.005	0	0
P_3	Wet	No	-0.026 (0.056)	41	0.18	-0.005	68	-0.008
P_4	Wet	Yes	0.075 (0.040)	116	0.50	0.038	89	0.029
TOTAL				231		-0.008	231	-0.029

(β_T) = effect size of T_{max} *in the model of nestling TL;* $N_{current}$*:* number of nestlings in each water availability condition in our dataset, $P_{current}$*:* proportion of nestlings in each water availability condition in our dataset, N_{future}*:* projected number of nestlings in each climate condition according to the projected changes in rainfall.

Population generation time.

The population of purple-crowned fairy-wrens studied is highly philopatric and isolated allowing for complete estimates of lifetime reproductive success and survival (44). For the population persistence modelling, we estimated generation time (T) using an equation from (45):

$$T = a + \frac{s}{(1 - s)}$$

Using data from Eastwood et al. (44), the mean age females achieved a breeding position was a = 1.254 years. Survival was calculated for each year in the study (44). Annual breeding female survival was then averaged (s = 0.792). Therefore, generation time was estimated to be T = 5.065.

Early-life telomere length association with lifetime reproductive success.

Table S4: Re-estimating the effect of telomere length on fitness to generate estimates on the appropriate scale for use in the evolutionary models. Shown are outcomes of a linear regression between telomere length (TL) and lifetime reproductive success (LRS) among birds that survived to reach a breeding position. Bold font denotes P <0.05. This model is the same as Table S3 in Eastwood et al. (44), except that here telomere length is z-score transformed, LRS is expressed as number of offspring that gain a breeder position instead of number of offspring that reach independence, and linear regression replaces a negative binomial model (since the model in Box 1 requires a linear estimate; the correlation between linear regression and negative binomial model predicted values was 0.99). See Eastwood et al. (44) for a full description of methods.

Dependent variable	Climate model notation	Independent variable	β (SE)	95 % CI lower	95 % CI upper	t	*p* value
Lifetime reproductive success (*n* = 43)	$\overline{W}_0$	intercept	1.131 (0.336)	0.453	1.810	3.369	0.002
	β_W	**TL (z-score)**	**0.518 (0.252)**	**0.009**	**1.028**	**2.055**	**0.047**
		sex (male)*	-0.178 (0.505)	-1.198	0.842	-0.353	0.726

*compared to female

Telomere length heritability.

To estimate heritability in telomere length we used a complete pedigree for our population (46) and mixed models in a Bayesian framework implemented with the package "MCMCglmm" (Hadfield 2010). Random effects included nest identity ((47) to account for common nest environment), pedigree data (to estimate the additive genetic variance), qPCR RunID (to account for between-qPCR plate variability in telomere estimates) and year. We ran two models with different fixed effect structures: the first one only included storage buffer (two levels: Ethanol and Longmire's buffer) as a fixed effect since this can affect telomere length (5). The second one included this parameter but also nestling age (as telomere length declines in early age) and sex (8). Model chains were ran for 3005000 iterations per model, from which we discarded the initial 5000 (burn-in period) and sampled every 1000 iteration (thin interval). This yielded effective sample sizes of >1000 for each parameter. Fixed effect priors were normally distributed and centred on zero with large variances (default priors in MCMCglmm). Relatively un-informative prior settings were used for the residuals and random effects (list(G=list(G1= list(V=1, nu=1, alpha.mu = 0, alpha.V = 1000), G2=list(V=1, nu=1, alpha.mu = 0, alpha.V = 1000), G3=list(V=1, nu=1, alpha.mu = 0, alpha.V = 1000), G4=list(V=1, nu=1, alpha.mu = 0, alpha.V = 1000)), R=list(V=1, nu=0.002))). Posterior means and 95% credible intervals (CI) were estimated across the thinned samples for heritabilities (i.e., additive genetic variance to total phenotypic variance ratios) and other variance components. Full model results are depicted in Table S5. Telomere heritability was obtained as the variance explained by the pedigree divided by the total variance of all random factors plus the residual variance. For both models, heritability of telomere length was similar (h^2 model 1: posterior mean = 0.359, 95% credible interval = 0.084–0.659; h^2 model 2: posterior mean: = 0.376, 95% credible interval: 0.088–0.675). In separate models, we also calculated heritabilities for each sex to identify whether nestling TL heritability differed between the sexes. While males (h^2=0.4, 95%CI = 0.098 – 0.693) tend to have higher heritabilities than females (h^2=0.32, 95%CI = 0.065 – 0.624) both distributions overlap broadly.

Table S5: Bayesian mixed animal models to compute telomere heritability. Model 1 only includes storage buffer as fixed effect while model 2 also includes nestling age at sampling and sex. Variance associated with the pedigree is represented by the term 'Animal' while qPCR Run ID, year and Nest ID represent variance associated with qPCR assay (TL and GAPDH, cohort and nest of origin respectively).

Model	Effect/variances	Posterior mean	Lower 95%CI	Upper 95%CI	p-value
Model 1	**Fixed effects**				
	Intercept	-0.424	-1.700	0.534	0.540
	Blood storage buffer (Longmire's)	1.010	-0.301	2.370	0.164
	Variance components				
	Animal	0.680	0.313	0.995	
	qPCR Run ID	0.272	0.089	0.502	
	Year	1.280	7.58E-06	4.380	
	Nest ID	0.107	5.78E-06	0.213	
Model 2	**Fixed effects**				
	Intercept	-0.450	-1.682	0.559	0.483
	Sex (male)	0.137	-0.006	0.292	0.076
	Blood storage buffer (Longmire's)	0.924	-0.305	2.339	0.200
	Sampling age	0.013	-0.096	0.115	0.813
	Variance components				
	Animal	0.684	0.305	0.995	
	qPCR Run ID	0.273	0.084	0.494	
	Year	1.080	4.94E-08	3.850	
	Nest ID	0.117	2.94E-06	0.232	

Simulated parameter distributions.

We evaluated the models using 10^6 simulated parameter sets with parameter values drawn independently from normal distributions with the mean corresponding to the mid-point of the 95% confidence interval for the parameter, and standard deviation corresponding to a quarter of the difference between the upper and lower 95% CI (*i.e.*, 95% of the density of normally distributed random variables is within two standard deviations of the mean). See Fig. S4 for the distributions of simulated parameter values.

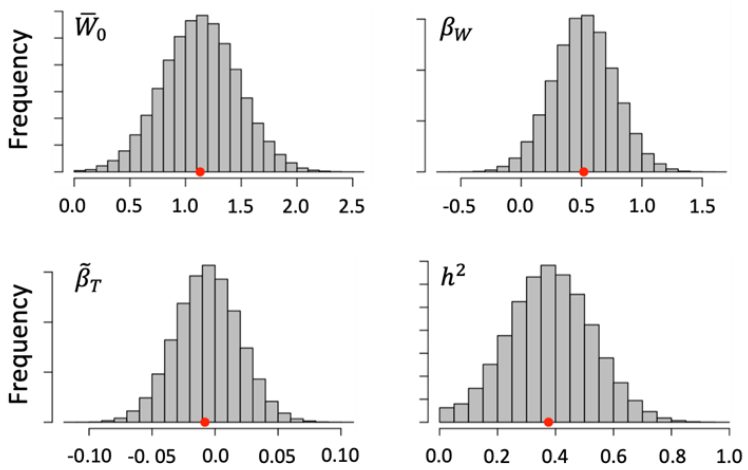

Figure S4. Simulated distributions of plausible parameter values for contemporary mean fitness of the population $\bar{W}_0$, the regression of reproductive success on telomere length β_W, the regression of telomere length on temperature β_T, and heritability of telomere length h^2, given the uncertainty in parameter estimates. Point estimate of parameters are shown in red. The distributions of simulated values are shown in grey. Since fitness cannot be negative and heritability is bounded between zero and one, we set negative parameter draws for $\bar{W}_0$ and h^2 to zero; draws of $h^2 > 1$ were set to one.

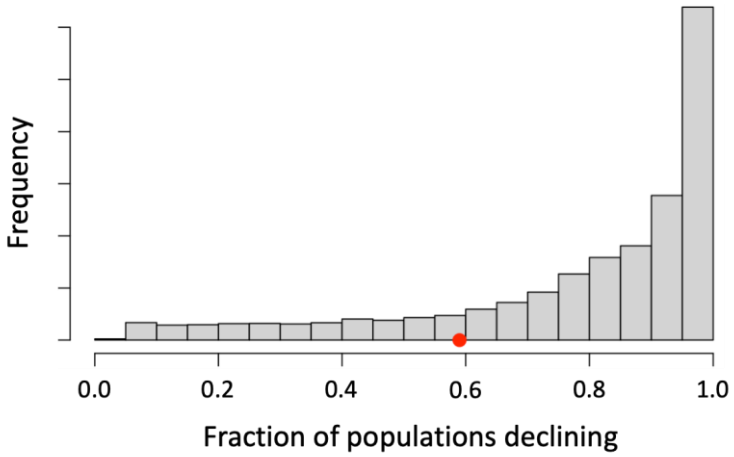

Figure S5: Simulations are skewed towards declining. Proportion of simulated populations that decline when proportions of the four environmental conditions are chosen at random. Results show proportions for 10,000 random sets for p_1, p_2, p_3, and p_4. The red circle shows the prediction based on the current empirically estimated values for p_1, p_2, p_3, and p_4 (*i.e.*, 59%).

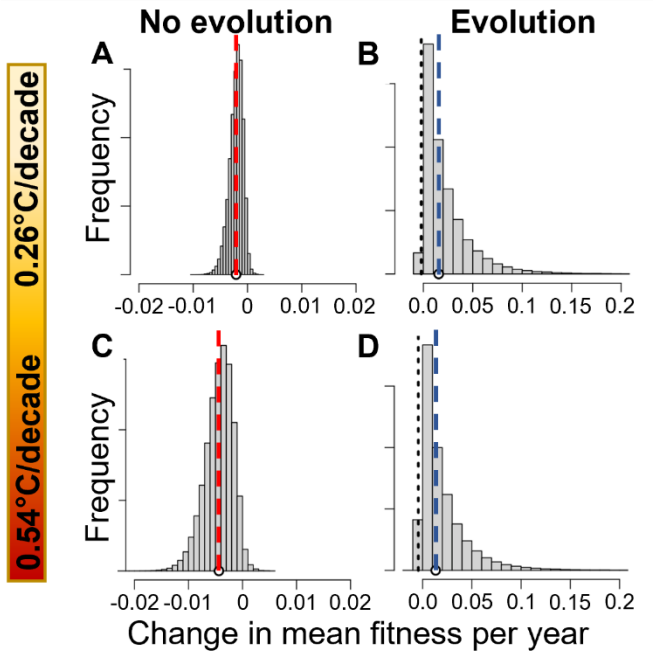

Figure S6. Modelling the worst-case scenario with and without evolution: the sublethal effects of climate warming on telomere length (TL) reduce fitness and force the population to decline in 98% of simulations. However, even the worst-case scenario can still be counteracted by adaptive evolution. Model and simulations are those described in Box 1. Panel A and B assumed an intermediate warming scenario (RCP4.5), panel C and D a high rate of warming (RCP8.5). Panel A and C depict outcomes of models without adaptive evolution of TL (zero heritability), whilst panel B and D depict model outcomes when assuming TL shows adaptive evolution (based on estimated links to fitness and heritability). Models take into account uncertainty in parameter estimates; dashed lines represent the values predicted using point estimates of the parameters with red for negative values and blue for positive values.

(VIII) Supplementary references

1. S. A. Kingma, M. L. Hall, A. Peters, A. E. A. Qvarnström, E. J. L. Bronstein, Multiple Benefits Drive Helping Behavior in a Cooperatively Breeding Bird: An Integrated Analysis. *Am. Nat.* **177**, 486–495 (2011).

2. N. H. Hidalgo Aranzamendi, M. L. Hall, S. A. Kingma, M. van de Pol, A. Peters, Rapid plastic breeding response to rain matches peak prey abundance in a tropical savanna bird. *J. Anim. Ecol.* **88**, 1799–1811 (2019).

3. N. Teunissen, S. A. Kingma, A. Peters, Nest defence and offspring provisioning in a cooperative bird: individual subordinates vary in total contribution, but no division of tasks among breeders and subordinates. *Behav. Ecol. Sociobiol.* **74**, 94 (2020).

4. M. J. Roast, *et al.*, Short-Term Climate Variation Drives Baseline Innate Immune Function and Stress in a Tropical Bird: A Reactive Scope Perspective. *Physiol. Biochem. Zool.* **92**, 140–151 (2019).

5. J. R. Eastwood, E. Mulder, S. Verhulst, A. Peters, Increasing the accuracy and precision of relative telomere length estimates by RT qPCR. *Mol. Ecol. Resour.* **18**, 68–78 (2018).

6. F. Criscuolo, *et al.*, Real-time quantitative PCR assay for measurement of avian telomeres. *J. Avian Biol.* **40**, 342–347 (2009).

7. E. Atema, K. van Oers, S. Verhulst, GAPDH as a Control Gene to Estimate Genome Copy Number in Great Tits, with Cross-Amplification in Blue Tits. *Ardea* **101**, 49–54 (2013).

8. P. Monaghan, S. E. Ozanne, Somatic growth and telomere dynamics in vertebrates: relationships, mechanisms and consequences. *Philos. Trans. R. Soc. Lond. B Biol. Sci.* **373**, 20160446 (2018).

9. R. A. Risques, D. E. L. Promislow, All's well that ends well: why large species have short telomeres. *Phil. Trans. R. Soc. B* **373**, 20160448 (2018).

10. E. L. B. Barrett, D. S. Richardson, Sex differences in telomeres and lifespan. *Aging Cell* **10**, 913–921 (2011).

11. S. A. Kingma, M. L. Hall, E. Arriero, A. Peters, Multiple benefits of cooperative breeding in purple-crowned fairy-wrens: a consequence of fidelity? *J. Anim. Ecol.* **79**, 757–768 (2010).

12. S. A. Kingma, M. L. Hall, A. Peters, No evidence for offspring sex-ratio adjustment to social or environmental conditions in cooperatively breeding purple-crowned fairy-wrens. *Behav. Ecol. Sociobiol.* **65**, 1203–1213 (2010).

13. N. Teunissen, S. A. Kingma, M. Fan, M. J. Roast, A. Peters, Context-dependent social benefits drive cooperative predator defense in a bird. *Curr. Biol.* **31**, 4120-4126.e4 (2021).

14. N. Teunissen, S. A. Kingma, A. Peters, Predator defense is shaped by risk, brood value and social group benefits in a cooperative breeder. *Behav. Ecol.* **31**, 761–771 (2020).

15. C. K. Cornwallis, *et al.*, Cooperation facilitates the colonization of harsh environments. *Nat. Ecol. Evol* **1**, 1–10 (2017).

16. W. Jetz, D. R. Rubenstein, Environmental Uncertainty and the Global Biogeography of Cooperative Breeding in Birds. *Curr. Biol.* **21**, 72–78 (2011).

17. A. R. Bourne, S. J. Cunningham, C. N. Spottiswoode, A. R. Ridley, Hot droughts compromise interannual survival across all group sizes in a cooperatively breeding bird. *Ecol. Lett.* **23**, 1776–1788 (2020).

18. D. Nettle, P. Monaghan, W. Boner, R. Gillespie, M. Bateson, Bottom of the Heap: Having Heavier Competitors Accelerates Early-Life Telomere Loss in the European Starling, Sturnus vulgaris. *PLoS ONE* **8**, e83617 (2013).

19. D. Nettle, *et al.*, An experimental demonstration that early-life competitive disadvantage accelerates telomere loss. *Proc. Royal Soc. B* **282**, 20141610 (2015).

20. J. J. Boonekamp, G. A. Mulder, H. M. Salomons, C. Dijkstra, S. Verhulst, Nestling telomere shortening, but not telomere length, reflects developmental stress and predicts survival in wild birds. *Proc. Royal Soc. B* **281**, 20133287 (2014).

21. P. J. J. Becker, *et al.*, Mother–offspring and nest-mate resemblance but no heritability in early-life telomere length in white-throated dippers. *Proc. Royal Soc. B* **282**, 20142924 (2015).

22. C. Bauch, J. J. Boonekamp, P. Korsten, E. Mulder, S. Verhulst, Epigenetic inheritance of telomere length in wild birds. *PLOS Genet.* **15**, e1007827 (2019).

23. E. Atema, *et al.*, Heritability of telomere length in the Zebra Finch. *J. Ornithol.* **156**, 1113–1123 (2015).

24. H. L. Dugdale, D. S. Richardson, Heritability of telomere variation: it is all about the environment! *Philos. Trans. R. Soc. Lond. B Biol. Sci.* **373**, 20160450 (2018).

25. S. A. Kingma, M. L. Hall, A. Peters, No evidence for offspring sex-ratio adjustment to social or environmental conditions in cooperatively breeding purple-crowned fairy-wrens. *Behav. Ecol. Sociobiol.* **65**, 1203–1213 (2010).

26. I. Rowley, E. Russell, The Purple-crowned Fairy-wren *Malurus coronatus*. II. Breeding Biology, Social Organisation, Demography and Management. *Emu* **93**, 235–250 (1993).

27. N. Hidalgo Aranzamendi, M. L. Hall, S. A. Kingma, P. Sunnucks, A. Peters, Incest avoidance, extrapair paternity, and territory quality drive divorce in a year-round territorial bird. *Behav. Ecol.* **27**, 1808–1819 (2016).

28. N. Hidalgo Aranzamendi, "Life-history variation in a tropical cooperative bird: Ecological and social effects on productivity," Monash University, School of Biological Sciences, Victoria, Australia. (2016).

29. S. Nolazco, M. L. Hall, S. A. Kingma, K. Delhey, A. Peters, No evidence for an adaptive role of early molt into breeding plumage in a female fairy wren. *Behav. Ecol.* **31**, 411–420 (2020).

30. M. Fan, *et al.*, From ornament to armament or loss of function? Breeding plumage acquisition in a genetically monogamous bird. *J. Anim. Ecol.* **87**, 1274–1285 (2018).

31. M. Fan, L. D'alba, M. D. Shawkey, A. Peters, K. Delhey, Multiple components of feather microstructure contribute to structural plumage colour diversity in fairy-wrens. *Biol. J. Linn. Soc.* **128**, 550–568 (2019).

32. D. L. Cram, P. Monaghan, R. Gillespie, T. Clutton-Brock, Effects of early-life competition and maternal nutrition on telomere lengths in wild meerkats. *Proc. Royal Soc. B* **284**, 20171383 (2017).

33. S. J. Cunningham, J. L. Gardner, R. O. Martin, Opportunity costs and the response of birds and mammals to climate warming. *Front. Ecol. Environ.* **19**, 300–307.

34. S. A. Kingma, M. L. Hall, E. Arriero, A. Peters, Multiple benefits of cooperative breeding in purple-crowned fairy-wrens: a consequence of fidelity? *J. Anim. Ecol.* **79**, 757–768 (2010).

35. L. Brouwer, *et al.*, Multiple hypotheses explain variation in extra-pair paternity at different levels in a single bird family. *Mol. Ecol.* **26**, 6717–6729 (2017).

36. M. L. Hall, A. Peters, Do male paternity guards ensure female fidelity in a duetting fairy-wren? *Behav. Ecol.* **20**, 222–228 (2009).

37. S. A. Kingma, M. L. Hall, A. Peters, Breeding synchronization facilitates extrapair mating for inbreeding avoidance. *Behav. Ecol.* **24**, 1390–1397 (2013).

38. G. E. Walsberg, W. W. Weathers, A simple technique for estimating operative environmental temperature. *J. Therm. Biol.* **11**, 67–72 (1986).

39. G. S. Bakken, Measurement and Application of Operative and Standard Operative Temperatures in Ecology. *Am. Zool.* **32**, 194–216 (1992).

40. S. J. Cunningham, R. O. Martin, P. A. Hockey, Can behaviour buffer the impacts of climate change on an arid-zone bird? *Ostrich* **86**, 119–126 (2015).

41. T. R. Cook, *et al.*, Parenting in a warming world: thermoregulatory responses to heat stress in an endangered seabird. *Conserv. Physiol.* **8**, coz109 (2020).

42. K. L. du Plessis, R. O. Martin, P. A. R. Hockey, S. J. Cunningham, A. R. Ridley, The costs of keeping cool in a warming world: implications of high temperatures for foraging, thermoregulation and body condition of an arid-zone bird. *Glob. Change Biol.* **18**, 3063–3070 (2012).

43. A. Moise, *et al.*, "Monsoonal North Cluster Report" in *Climate Change in Australia Projections for Australia's Natural Resource Management Regions: Cluster Reports*, M. Ekström, *et al.*, Eds. (CSIRO and Bureau of Meteorology, Australia, 2015).

44. J. R. Eastwood, *et al.*, Early-life telomere length predicts lifespan and lifetime reproductive success in a wild bird. *Mol. Ecol.* **28**, 1127–1137 (2019).

45. B.-E. Sæther, *et al.*, Generation time and temporal scaling of bird population dynamics. *Nature* **436**, 99–102 (2005).

46. M. Fan, M. L. Hall, M. Roast, A. Peters, K. Delhey, Variability, heritability and condition-dependence of the multidimensional male colour phenotype in a passerine bird. *Heredity* **127**, 300–311 (2021).

47. J. J. Wiens, Climate-Related Local Extinctions Are Already Widespread among Plant and Animal Species. *PLOS Biol.* **14**, e2001104 (2016).